Finite Element Modeling of RMS Roughness Effect on the Contact Stiffness of Rough Surfaces

M.B. Amor[a], S. Belghith[a], S. Mezlini[a]

[a]*Laboratoire Génie Mécanique, École Nationale d'Ingénieurs de Monastir, Université de Monastir, Tunisie.*

Corresponding author:

Saoussen Belghith
Laboratoire Génie Mécanique,
École Nationale d'Ingénieurs de Monastir,
Université de Monastir, Tunisie.
E-mail: belghith.saoussen@gmail.com

A B S T R A C T

The present study considers finite element analysis of an elastic and elastic-plastic contact between a rigid flat and a real rough surface taking into account the asperities interaction. Numerical modeling and measurement of the normal interfacial stiffness were conducted. Surfaces with different rms roughness values were investigated in the elastic and power-law hardening models to highlight the combined effect of the topography and the strain hardening on the contact characteristics. The influence of the surface roughness on the interaction between neighboring micro-contacts, the residual stress and deformation for the power-law hardening material was analyzed. The obtained results have shown the importance of considering the strain hardening in the modeling of a rough contact especially for rougher surface.

1. INTRODUCTION

Understanding the contact mechanics between engineering surfaces is a requirement for many technological applications involving friction, wear, lubrication and conduction of heat and electricity between solids. In reality, all engineering surfaces are rough. When they are pressed together, real contact occurs particularly at few peaks especially at low pressure. The surface topography is therefore of great interest to control tribological and mechanical behavior in the contact.

A review of the literature reveals several approaches for predicting rough surface performances. The classical statistical approach firstly built by Greenwood and Williamson [1] based on various restricted assumptions was widely used on contact analysis [2–6]. The Greenwood and Williamson model (GW model) assumed that all surface asperities are identical hemispheres with the same curvature radius and Gaussian height distribution. The contact zones are dispersed and the asperity deformation is independent of its neighboring. In spite of these assumptions, the GW model gives reliable results [7]. Many attempts were later made to extend the GW model to elastic-plastic behavior notably the Chang, Etsion and Bogy [2] and the Kogut and Etsion [8] models. In all these models the bulk deformation was always neglected so no interactions between neighboring contacting asperities are taken into account [9]. Therefore, only few analytical models have been developed considering the

interaction between asperities in elastic-plastic contact [10,11].

Later, another approach has been proposed by Archard [12], applied subsequently by Majumdar and Bhushan [13] and then by Persson [14]. This approach was based upon the multi-scale nature of the surfaces, where each asperity has smaller asperities on its surface at all scales. This description of rough surfaces was mathematically written using the self-affinity fractal concept [13,14]. A number of numerical models of elastic [15–17] and elastic-plastic [18,19] of rough contact were performed considering the self-affinity of rough surfaces. In a noteworthy study, Hyun et al. [15] developed a three dimensional elastic contact model with a range of self-affine fractal scaling behavior. They found a linear proportionality between real area and contact load at small loads. The mean pressure is shown to be independent to load, whereas it is proportional to the root mean square (rms) surface slope. In order to improve their previous model, Pei, Hyun et al. [18] extend the elastic model [15] to an elastic-plastic one considering wider range of self-affine fractal topography and varying material properties. They showed that the range of proportionality between area and load in the elastic-plastic contact is wider than that for the elastic case. Afterwards, Sahoo and Ghosh [19] have conducted a finite element contact analysis of elastic and elastic-plastic fractal surfaces using a commercial finite element software. This model studied the influence of variable fractal dimension D and fractal roughness parameter G in the case of elastic contact and variable rates of strain hardening in the case of elastic-plastic contact. A linear load-area relationship was found for both elastic and elastic-plastic surfaces. For the elastic surfaces the linearity is limited to small load range and rougher surfaces. In the elastic-plastic model the load-area relationship is also linear for different rates of strain hardening except for perfectly elastic-plastic behavior where bilinear relationship was found.

In addition, several numerical models of elastic-plastic [9,20–24] rough contact investigate real profiles measured from engineering surfaces with realistic material behavior. Zhao et al. [9] developed a finite element power-law hardening model of a rough surface which takes into account the asperities interaction effect. The measured profile was simplified and reconstructed to be accurately simulated. They proved that the power-law hardening properties, strain hardening exponent and the ratio of Young's modulus to yield strength, greatly affect the asperity interaction. In addition, Chatterjee and Sahoo [24] investigated the effect of strain behavior and hardening law in shakedown behavior using ANSYS software under full stick contact. Repeated normal loading unloading of elastic plastic sphere against a rigid flat specimen has been simulated with varying tangent modulus. It was found that with small tangent modulus the cyclic loading process gradually converges into elastic shakedown. The effect of strain hardening laws on shakedown behavior is pronounced at high tangent modulus.

In same cases of machining process the generated surface topography satisfied the requirements of the 2D simplification assumption [20–33]. Westergaard [25] is the first who solved the perfectly elastic two-dimensional sinusoidal contact. Recently, Gao et al. [26] and Manners [27] provided two-dimensional sinusoidal contact model considering elastic-plastic behavior and using a finite element method. Their results were in agreement with those obtained using a three dimensional model of contact of sinusoidal surfaces [26,27] which encouraged other researches to investigate two-dimensional modeling. More recently, the two dimensional plane strain model was used to modulate the rolling/sliding behavior of a wheel rolling on a rail [19,20]. This model considers roughness of the contact surfaces having an elastic-plastic behavior. Using sinusoidal topography for the rail and smooth surface for the wheel, the surface deformation was evaluated.

Belghith et al. [22] have, also, developed a two dimensional thermo-mechanical model of contact between rough surfaces. Realistic profiles were analyzed by the finite element model with an elastic-plastic material behavior and the asperities interaction was inherently considered. This model allows the analysis of the real contact area and thermal contact resistance. Interestingly, Bryant et al. [23] developed a 2D finite element analysis of an elementary contact (line contact) between quarter cylinder and a rigid plane. Multiple contacts were analyzed by modeling a contact between a sinusoidal surface

and a rigid plane and a relevant comparison with the work of Westergaard [25] was carried out.

The present work aims to analyze numerically the combined effect of roughness and deformation mode, purely elastic or elastic-plastic, on the contact performances. A power-law hardening material was used since it is more appropriate to deal with realistic material properties. The asperities interaction was inherently considered and discussed for the elastic-plastic contact. This study was applied to a rough contact between real profile and rigid plan from infinitesimal to almost full contact. Contact characteristics such as real area of contact and normalized load are illustrated considering different rms roughnesses. The study is also focused on the finite element modeling and measurement of the normal contact stiffness of rough surfaces in the elastic and power-law hardening model. The effect of roughness on the Von Mises and the residual stress after the unloading process is also shown.

2. TOPOGRAPHIC PROPERTIES OF THE INVESTIGATED PROFILES

In order to analyse the mechanical behaviour of a rough contact, a profile of a rough surface were experimentally measured using a stylus profile instrument and respecting the rules of measurements defined by the standardized method ISO 4288. The measured profile was filtered (Fig. 1) and roughness parameters were calculated using the standardized method ISO 4287 frequently used in the literature in order to evaluate the performances of a rough contact.
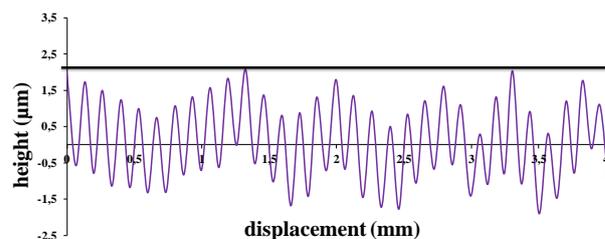

Fig. 1. Investigated contact: Surface profile-flat plan.

Table 1. Statistical parameters of the investigated profiles.

Profiles	1	2	3	4	5
R_q (µm)	1.23	1.84	2.46	3.08	3.69
Δ_a(°)	0.034	0.051	0.068	0.085	0.102
Δ_q(°)	0.005	0.008	0.011	0.013	0.016

In order to study the effect of roughness parameters on the mechanical behavior of contacting rough surfaces, the considered profile was artificially modified by multiplying its summits and valleys heights by 1.5, 2, 2.5 and 3 to produce four other profiles. The resulting profiles have the same spacing parameters and different values of the central line average R_a, the rms roughness R_q, the average and the rms slope Δ_a and Δ_q respectively. This allows to analyse the influence of these amplitude parameters on the rough surface behavior. The same values of the skewness (R_{sk}=0) and kurtosis (R_{ku}=1.5) are kept constant for all the generated profiles to remove the effects of the symmetry and the flatness of the height distribution. The studied profiles are named respectively 'profile 1', 'profile 2', 'profile 3', 'profile 4', and 'profile 5' (Fig. 2). The roughness parameters describing the generated profiles are given in Table 1.
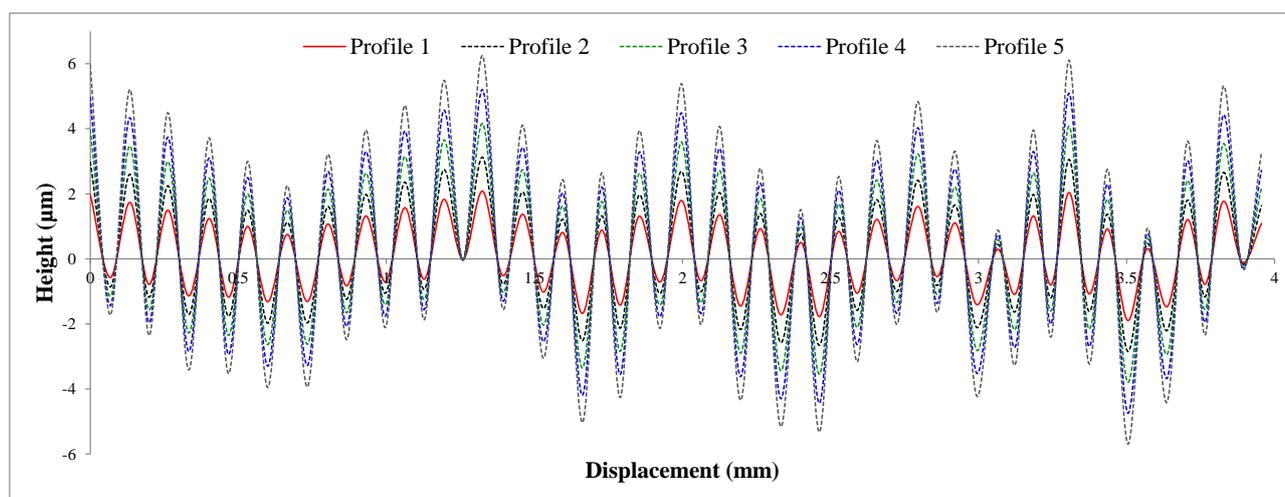

Fig. 2. Profiles of the simulated rough surfaces.

3. FINITE ELEMENT MODEL

In this section, a 2D plane strain model was developed on the microscopic scale to study the performance of a rough contact. This configuration is relevant in several cases where the surface topography satisfies the requirements of the 2D simplification, as the case of hardened and ground gears [22]. Firstly, an elastic contact was studied. Then, an elastic-plastic contact model was developed using a power hardening law. The effect of the amplitude parameters on the contact behaviour in both elastic and elastic-plastic model was analysed. A commercial finite element solver, ABAQUS/Standard was used in the present work. A schematic representation of the established model which shown the different parts, dimensions and boundary conditions is given in Fig. 3. The upper body (Body1) illustrates the smooth rigid surface, while the lower one (Body 2) is the deformable rough body. The upper surface of the latter was shaped by introducing the profiles, described previously, from 1 to 5 consecutively. To do this a coupling between the ABAQUS software and the Python script was used.
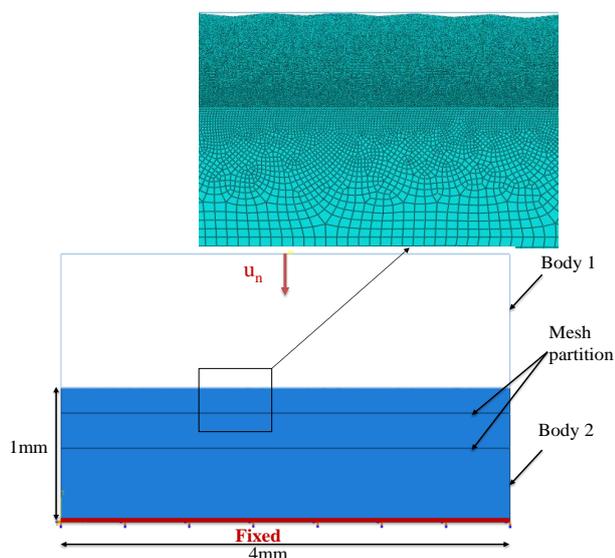

Fig. 3. Profiles of the simulated rough surfaces.

The boundary conditions for Body 2 are prescribed by fixing its bottom and keeping lateral sides free of constraints. The normal load was accomplished by applying to the rigid plan a normal displacement (u_n). Linear plane strain elements are used to mesh body 2. Using the partitioning tool, the model was divided into three partitions with different meshes with different element shape and size. Near the surface roughness, the mesh was triangular

(CPE3) sufficiently refined to allow the surface irregularities to be covered and accurately simulated. The number of elements along the interface increases with the degree of roughness. Quadrilateral (CPE4R) and larger elements are used throughout the two other partitions to minimize the calculation time. Mesh tests were performed to determine the sensitivity of the data to a variation in the mesh size.

The interaction between surfaces was defined using the *Surface to Surface* algorithm and *finite sliding formulation*. The tangential behavior was governed by the Penalty contact method. This model allows solving the nonlinear contact problem since it accounts the geometric nonlinearity (Large-displacement formulation) and the elastic-plastic material behavior.
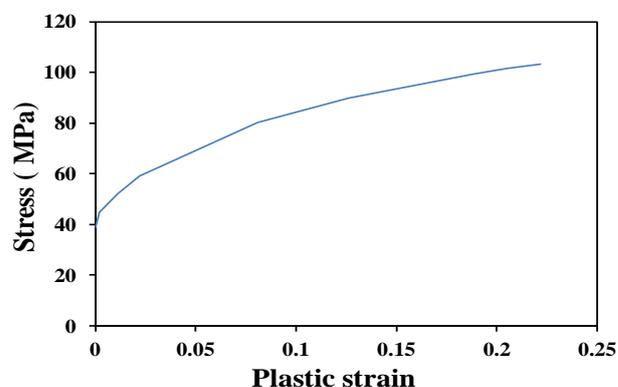

Fig. 4. The power-law hardening curve.

In the elastic model, the material behavior is described by the equivalent Young's modulus and the Poisson coefficient (Young modulus of 70 GPa and Poisson ratio of 0.3). In the elastic-plastic model, the material's behaviour of the rough surface is considered using large deformation and elastoplastic theory. More specifically, the plastic flow is described via the Von Mises plasticity criterion. The material's elastic characteristics used previously have been taken. A non-linear elastoplastic behaviour has been added (Fig 4).
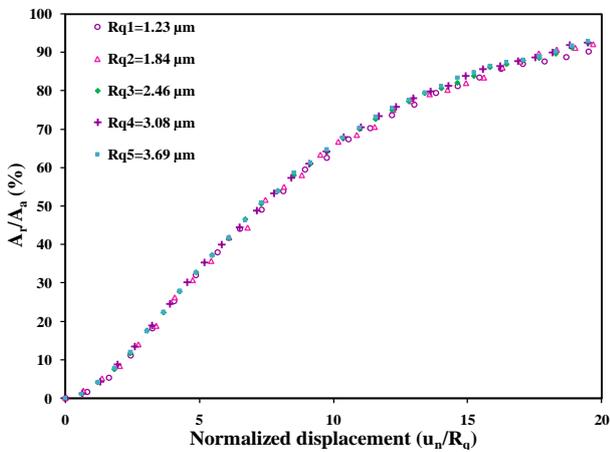
4. RESULTS AND DISCUSSION

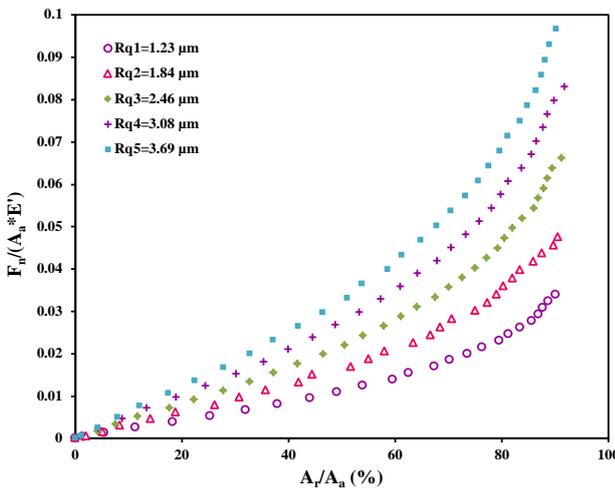### 4.1 Elastic rough contact model

Effect of the rms roughness on the contact area ratio and normalized load

The elastic contact analysis was firstly conducted based on the above described

numerical model. The effect of the rms variation on the mechanical behavior of rough surfaces has been investigated. The evolution of the contact area ratio (A_r/A_a) as a function of the normalized displacement (u_n/R_q) of the rigid plan for different rms roughness values was shown in Fig. 5 (a) for different values of R_q. It can be seen from this figure that for purely elastic behavior the rms roughness have no observable effects on the evolution of the contact area ratio against the normalized displacement. This implies that the same normalized displacement (The same rate of roughness deformation) produces the same contact area ratio regardless of the surface amplitude parameters.

(a)

(b)

Fig. 5. (a) Contact area ratio versus normalized displacement, (b) Variation of normalized load with the contact area ratio.

Figure 5 (b) shows the plots of the dimensionless normal load $F_n/(A_a E')$ as a function of the contact area ratio. The numerical results corresponding to

the elastic surfaces with different rms roughnesses were presented. As can be seen, all the surfaces predict a linear relationship in a relatively wide range, this range is about 70 % of the apparent area for profile 1 and 50 % of the apparent area for profile 5. The constant of proportionality is found to be higher for a higher rms roughness. Consequently, for the same contact area an increase in the rms roughness leads to an increase in the load capacity. When the rms roughness is growing three times, the constant of proportionality will increase by the same factor. However, a growing deviation from linear fit can be noted at larger contact area for all curves. The increase of load is more important than the increase in the real area since the contact approaches the full contact conditions and the real area is almost equal to the apparent area.

Effect of the rms roughness on the normal contact stiffness

Based on the F.E.M, a methodology was developed for measuring the contact stiffness of the simulated rough solid. The deformation of the rough deformable body simulated by the F.E.M includes the bulk deformation and the interface (roughness) deformation. Thus a rough solid is described by the contact stiffness $K_{contact}$, the bulk stiffness K_{bulk}, and the overall stiffness K_{Total}. A parallel spring model was used to relate different normal stiffness describing the rough solid as follows [28].

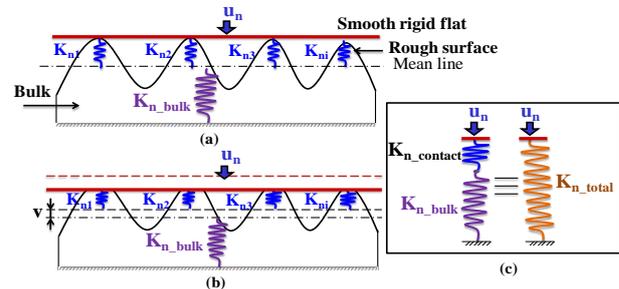$$\frac{1}{K_{n\_Total}} = \frac{1}{K_{n\_bulk}} + \frac{1}{K_{n\_contact}} \tag{1}$$

Fig. 6. Spring model representation: (a) before loading (b) after loading (c) equivalent rheological model.

Figure 6 illustrates a rheological modelling of the current F.E.M. Each asperity is modelled as a spring of stiffness K_{ni}. The bulk is modelled as a spring of stiffness K_{n_bulk}. The normal contact stiffness $K_{n\_contact}$ which characterize the interfacial rigidity is the equivalent stiffness

associated with all coupled springs K_{ni} throughout the rough interface. The total stiffness K_{n_total} which describes the rigidity of the entire deformable body was derived directly from the F.E.M (Eq. (2)).

$$\frac{1}{K_{n\_total}} = \frac{\partial F_n}{\partial u_n} \qquad (2)$$

The interfacial stiffness is only due to the displacement of the surface roughness. In order to calculate the interfacial stiffness, the displacement of the bulk (v) must be subtracted from the imposed displacement to determine the displacement of the surface roughness, called the normal approach (δ) (Eq. (3)). To calculate the displacement of the bulk, the position of the mean line of the profile was identified in each increment of loading by fitting the profile nodes using the least square method.

$$\delta = u_n - v \qquad (3)$$

The interfacial stiffness was calculated by differentiating the normal load F_n with respect to the normal approach δ (Eq. (4)).

$$\frac{1}{K_{n\_contact}} = \frac{\partial F_n}{\partial \delta} \qquad (4)$$

The bulk stiffness was calculated by differentiating the normal load F_n with respect to the displacement of the mean line (v) (Eq. (5)).

$$\frac{1}{K_{n\_bulk}} = \frac{\partial F_n}{\partial v} \qquad (5)$$

Example of the evolutions of $K_{n\_contact}$, K_{n_bulk} and K_{n_total} versus the nominal pressure P_n is presented in Fig. 7.
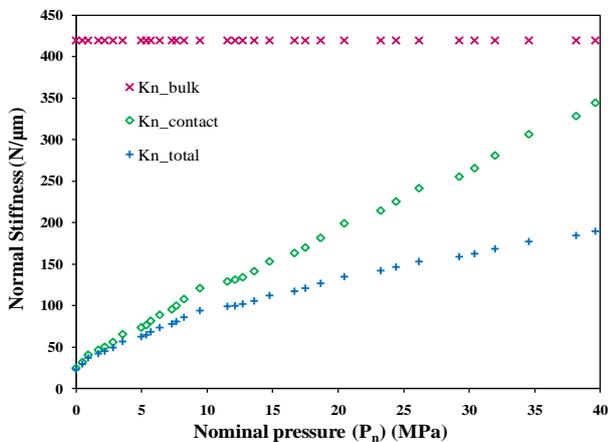

Fig. 7. Evolution of contact stiffness, bulk stiffness and total stiffness as a function of nominal pressure for profile 1.

It is seen that with increasing the applied pressure both the contact and total stiffness increase. It can be noted that the interfacial stiffness is almost linearly proportional to the applied load.
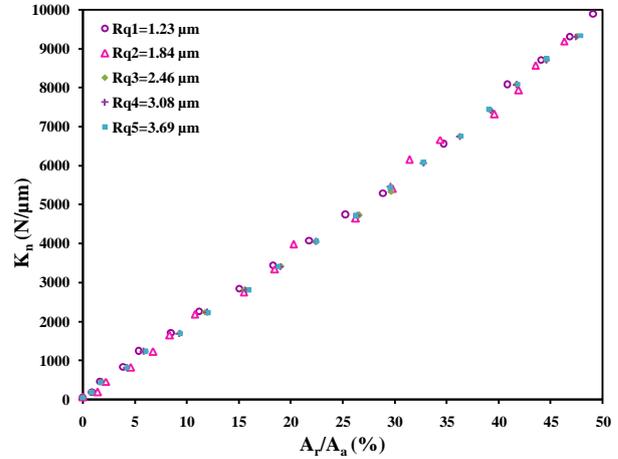

Fig. 8. Contact stiffness of elastic contact versus the area ratio.

Figure 8 shows the interfacial normal stiffness as a function of the contact area ratio. This figure exhibits approximately linear relationship between the normal contact stiffness and the real area which is in good agreement with results of S. Akarapu et al. [29]. Results show identical responses for different rms roughness values. Once again, the rms roughness does not appear to have any significant effect on the elastic contact stiffness curves which collapse to a single curve.

4.2. Elastic-plastic rough contact model: Power-law hardening material

Effect of the rms roughness on the contact area ratio and normalized load

Figure 9 (a) illustrates the influence of the rms roughness on the evolution of the real area with the normalized displacement for elastic-plastic contact. It is seen that at a particular normalized displacement the surface with the largest rms roughness has the highest contact area ratio. The increase of the rms roughness gives rise to growing strain hardening. In other words, the roughest surface presents sharper peaks which induced more yielding behaviour in the highest asperities tips compared to other surfaces. At a given normalized displacement, the asperities tips were plastically deformed, giving rise to a deformation resistance which is more significant

for the roughest surface. Thus, this surface induces higher contact force and higher real area of contact. As the normalized displacement increases, number and size of contact spots increase hence the real area of contact approaches to the nominal. Thus, at large normalized displacement, the rms roughness has no effect on the real contact area.
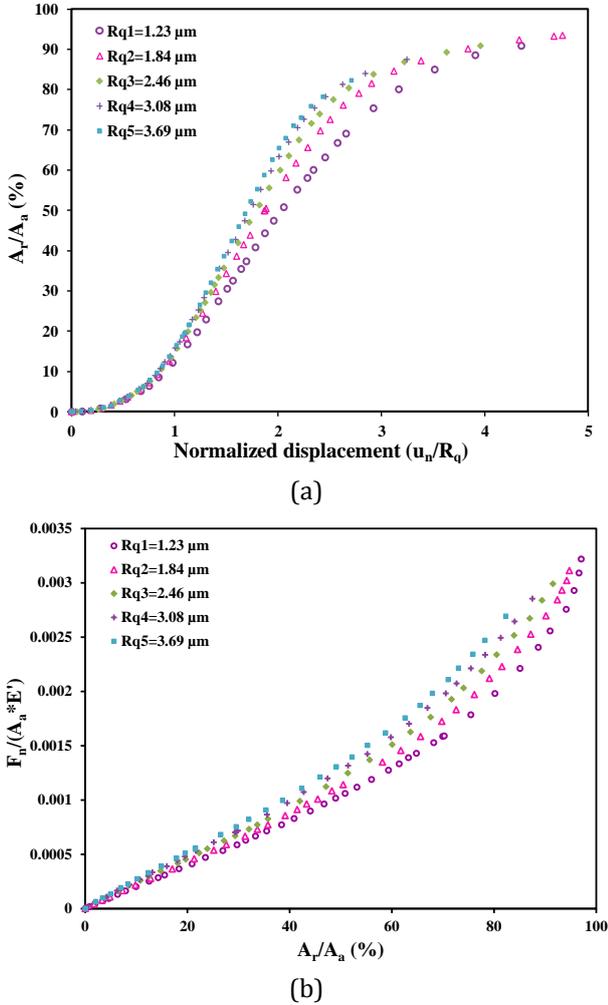

(a)

(b)

Fig. 9. (a) Variation of the area ratio with normalized displacement for the elastic-plastic model, (b) Normalized load versus contact area ratio.

The relationship between the real contact area and the dimensionless load was, equally, studied for the elastic-plastic contact considering the effect of rms roughness (Fig. 9 (b)). The dimensionless load increases linearly with the contact area ratio up to 60 %. At a particular area ratio, the load capacity is found to be most significant for the surface with the highest rms roughness. When the rms roughness increases three times, the constant of proportionality increases of about 30 %. It can be noted that the influence of the roughness parameters (R_q, Δ_q)

on the load capacity seems to be less pronounced when considering the hardening effect than the elastic case.

Effect of the rms roughness on the normal contact stiffness

The same methodology explained above was used to evaluate the contact stiffness. The combined effect of roughness and power-law hardening was also highlighted by evaluating the normal contact stiffness dependence on the contact area ratio (A_r/A_a) for different roughness level (Fig. 10). The normal contact stiffness rises almost linearly with the real area of contact. Numerical results reveal that for elastic plastic model, the rms roughness have a major effect on the normal contact stiffness contrary to what has been found for elastic case. The smoothest surface, with the lowest rms roughness, has the greater normal contact stiffness. For a fixed real area, an increase of the roughness parameter R_q leads to a decrease in the normal contact stiffness. These observations show the importance of elastic plastic behavior on the mechanical behavior of rough contact and in particular on its normal stiffness.
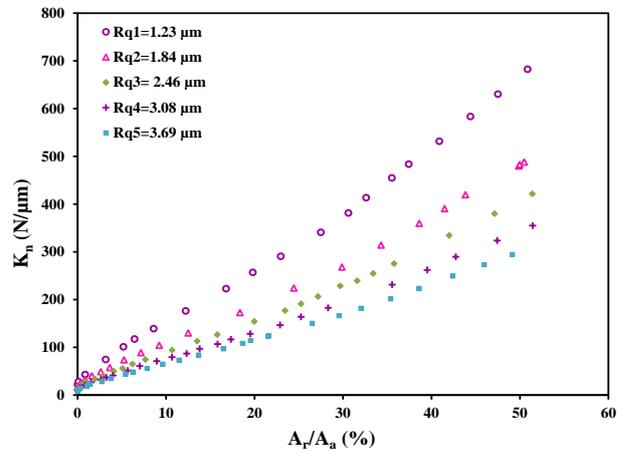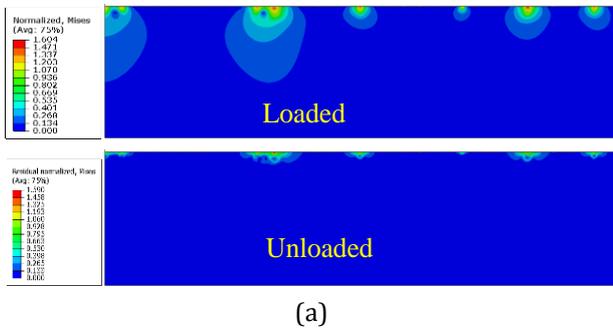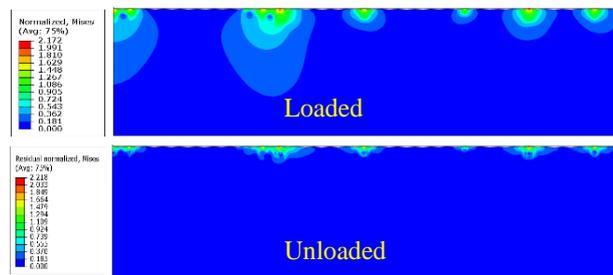

Fig. 10. Contact stiffness against area ratio for the elastic-plastic model.

In a further test, the investigated surfaces were successively loaded and unloaded. Figures 11-12 (a) show the distribution of the loaded Von Mises equivalent stress normalized by the yield stress for two extremes values of R_q at low and high deformations. It can be seen that even for relatively low deformation (u_n/R_q=0.5) neighboring asperities can slightly interact with each other. As the deformation increases, new asperities come into contact and micro-contacts

already present grow in size which leads to more interaction between asperities. For a fixed normalized displacement, the investigated profiles provide the same number of contacts, however, the size of micro-contacts grows with the rms roughness. Hence, the interaction is more pronounced for the highest rms roughness.
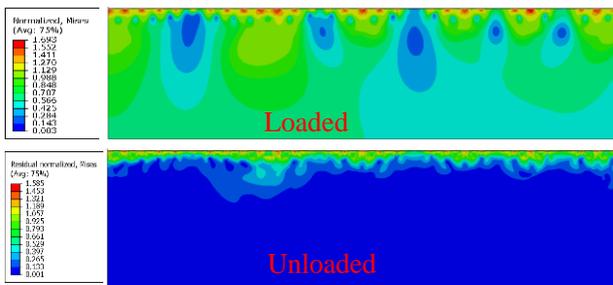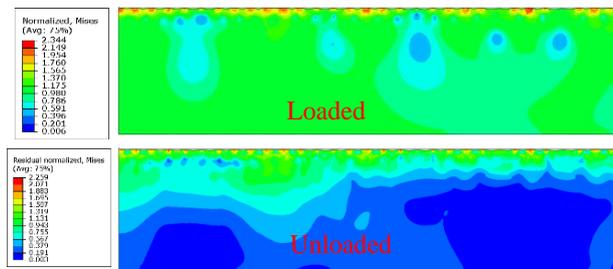

Fig. 11. Loaded and residual normalized Von Mises stress contours for u_n/R_q=0.5 : (a) R_q=1.23μm, (b) R_q= 3.69μm.

Fig. 12. Loaded and residual normalized Von Mises stress contours for u_n/R_q=1.5: (a) R_q=1.23μm, (b) R_q=3.69μm.

The normalized residual Von Mises yielding was used to detect area of the irreversible strain. For a particular normalized displacement, even though the same asperities come into contact regardless the R_q value, the roughest surface provides the highest residual stress. In the early contact the highest stress occurs locally in the tallest asperity which comes in contact first. As the load increases, the highest stress area moves and takes place in the next tallest asperity with relatively lower height and smaller width so higher slope than the tallest asperity. This suggests the influence of asperity slope on the values and distributions of residual stress.

5. CONCLUSION

A numerical model was developed for 2D roughness profile with the finite element method to investigate the mechanical behaviour of a rough contact. This investigation has employed real profiles and the asperities interaction was considered. Elastic contact model was built at first. This model was extended to realistic elastic-plastic behaviour by involving power-law hardening material behaviour. An accurate modelling and measuring of the interfacial stiffness of real surfaces using finite element software was performed. The effect of rms roughness on the performances of elastic as well as elastic-plastic contact is analysed and the effect of plasticity is shown.

Based on the obtained results, the following conclusions can be retained:

1. In the case of purely elastic solids, at a given normalized displacement the rms roughness exhibits no effect on the real area of contact. However, in the power-law hardening model a rougher surface provides a higher real area of contact.

2. The elastic contact stiffness depends on the real area of contact but it is independent of the rms roughness. When the power-law hardening was involved, the interfacial stiffness is shown to be greatly sensitive to the rms roughness. The elastic-plastic contact stiffness is not uniquely dependent on the real area but also on the size, number and deformation pattern of spots into contact.

3. Both the elastic and elastic-plastic contact reveals linear relationship between load and real area at a relatively substantial range. Compared to the elastic model, the range of proportionality is greater for the elastic-plastic case. The deviation of the power-law hardening contact from purely elastic case is most notable for the roughest surface which incurs more plastic yielding.

4. The rms roughness greatly affects the asperities interaction and the residual deformation of the elastic-plastic surface. An increase of the rms roughness leads to more interaction between asperities and larger residual deformation.

5. Considering power-law hardening behaviour leads to a large deviation from the purely elastic contact at small and large deformation mostly for rougher surfaces. It is therefore important to take into account plasticity effects when modelling real rough contacts especially for high roughness.

REFERENCES

[1] J.A. Greenwoold and J.B.P. Williamson, "contact of normally flat surfaces," *Proc. R. Soc. Lond. Ser. A*, vol. 295, pp. 300–318, 1966.

[2] W.R. Chang, I. Etsion and D.B. Bogy, "An Elastic-Plastic Model for the Contact of Rough Surfaces," *Journal of Tribology*, vol. 109, no. 2. p. 257, 1987.

[3] D.J. Whitehouse and J.F. Archard, "The Properties of Random Surfaces of Significance in their Contact," *Proceedings of the Royal Society A: Mathematical, Physical and Engineering Sciences*, vol. 316, no. 1524. pp. 97–121, 1970.

[4] J.A. Greenwood and J.H. Tripp, "The Elastic Contact of Rough Spheres," *Journal of Applied Mechanics*, vol. 34, no. 1. p. 153, 1967.

[5] Y. Zhao, D.M. Maietta and L. Chang, "An Asperity Microcontact Model Incorporating the Transition From Elastic Deformation to Fully Plastic Flow," *Journal of Tribology*, vol. 122, no. 1. p. 86, 2000.

[6] S. Bhaumik, A. Kumaraswamy, S. Guruprasad and P. Bhandari, "Tribology in Industry Study of Effect of Seal Profile on Tribological Characteristics of Reciprocating Hydraulic Seals," *Tribol. Ind.*, vol. 37, no. 2, pp. 264–274, 2015.

[7] J.I. McCool, "Comparison of models for the contact of rough surfaces," *Wear*, vol. 107, no. 1, pp. 37–60, 1986.

[8] L. Kogut and I. Etsion, "A Finite Element Based Elastic-Plastic Model for the Contact of Rough Surfaces," *Tribol. Trans.*, vol. 46, no. 3, pp. 383–390, 2003.

[9] B. Zhao, S. Zhang and Z. Qiu, "Analytical asperity interaction model and numerical model of multi-asperity contact for power hardening materials," *Tribol. Int.*, vol. 92, pp. 57–66, 2015.

[10] Y. Zhao and L. Chang, "A Model of Asperity Interactions in Elastic-Plastic Contact of Rough Surfaces," *Journal of Tribology*, vol. 123, no. 4. p. 857, 2001.

[11] P. Sahoo and A. Banerjee, "Asperity interaction in elastic–plastic contact of rough surfaces in presence of adhesion," *Journal of Physics D: Applied Physics*, vol. 38, no. 16. pp. 2841–2847, 2005.

[12] J.F. Archard, "Elastic Deformation and the Laws of Friction," *Proceedings of the Royal Society A: Mathematical, Physical and Engineering Sciences*, vol. 243, no. 1233. pp. 190–205, 1957.

[13] A. Majumdar and B. Bhushan, "Role of Fractal Geometry in Roughness Characterization and Contact Mechanics of Surfaces," *Journal of Tribology*, vol. 112, no. 2. p. 205, 1990.

[14] B.N. Persson, "Elastoplastic contact between randomly rough surfaces.," *Phys. Rev. Lett.*, vol. 87, no. 11, p. 116101, 2001.

[15] S. Hyun, L. Pel, J.F. Molinari and M.O. Robbins, "Finite-element analysis of contact between elastic self-affine surfaces," *Phys. Rev. E - Stat. Nonlinear, Soft Matter Phys.*, vol. 70, no. 2 2, pp. 1–12, 2004.

[16] G.G. Batrouni, A. Hansen and J. Schmittbuhl, "Elastic response of rough surfaces in partial contact," *EPL (Europhysics Lett.*, vol. 60, no. 5, p. 724, 2002.

[17] M. Ciavarella, C. Murolo and G. Demelio, "On the elastic contact of rough surfaces: Numerical experiments and comparisons

with recent theories," *Wear*, vol. 261, no. 10, pp. 1102–1113, 2006.

[18] L. Pei, "WTC2005-63567 FINITE ELEMENT MODELING OF SLIDING CONTACT BETWEEN ROUGH SURFACES," pp. 2–3, 2005.

[19] P. Sahoo and N. Ghosh, "Finite element contact analysis of fractal surfaces," *J. Phys. D. Appl. Phys.*, vol. 40, no. 14, pp. 4245–4252, 2007.

[20] W.K. Kubin, M. Pletz, W. Daves and S. Scheriau, "A new roughness parameter to evaluate the near-surface deformation in dry rolling/sliding contact," *Tribol. Int.*, vol. 67, pp. 132–139, 2013.

[21] M. Pletz, W. Daves, W. Yao, W. Kubin and S. Scheriau, "Multi-scale finite element modeling to describe rolling contact fatigue in a wheel–rail test rig," *Tribol. Int.*, vol. 80, pp. 147–155, 2014.

[22] S. Belghith, S. Mezlini, H. Belhadjsalah and J. L. Ligier, "Thermo-mechanical modelling of the contact between rough surfaces using homogenisation technique," *Mech. Res. Commun.*, vol. 53, no. 1, pp. 57–62, 2013.

[23] M.J. Bryant, H.P. Evans and R.W. Snidle, "Plastic deformation in rough surface line contacts—a finite element study," *Tribol. Int.*, vol. 46, no. 1, pp. 269–278, 2012.

[24] B. Chatterjee and P. Sahoo, "Shakedown Behavior in Multiple Normal Loading - Unloading of an Elastic - Plastic Spherical Stick Contact," *Tribol. Ind.*, vol. 35, no. 1, pp. 3–18, 2013.

[25] H.M. Westergaard, "Bearing pressures and cracks," *J. Appl. Mech.*, vol. 61, pp. A49–A53, 1939.

[26] Y.F. Gao, A.F. Bower, K.-S. Kim, L. Lev and Y. T. Cheng, "The behavior of an elastic–perfectly plastic sinusoidal surface under contact loading," *Wear*, vol. 261, no. 2, pp. 145–154, 2006.

[27] W. Manners, "Plastic deformation of a sinusoidal surface," *Wear*, vol. 264, no. 1–2, pp. 60–68, 2008.

[28] V. Krithivasan and R.L. Jackson, "An analysis of three-dimensional elasto-plastic sinusoidal contact," *Tribol. Lett.*, vol. 27, no. 1, pp. 31–43, 2007.

[29] R.L. Jackson, V. Krithivasan and W.E. Wilson, "The pressure to cause complete contact between elastic–plastic sinusoidal surfaces," *Proc. Inst. Mech. Eng. Part J J. Eng. Tribol.*, vol. 222, no. 7, pp. 857–863, 2008.

[30] D.M. Mulvihill, H. Brunskill, M.E. Kartal, R.S. Dwyer-Joyce and D. Nowell, "A Comparison of Contact Stiffness Measurements Obtained by the Digital Image Correlation and Ultrasound Techniques," *Exp. Mech.*, vol. 53, no. 7, pp. 1245–1263, 2013.

[31] S. Akarapu, T. Sharp and M.O. Robbins, "Stiffness of contacts between rough surfaces," *Phys. Rev. Lett.*, vol. 106, no. 20, pp. 1–4, 2011.

[32] S. Roy and P. Sahoo, "Multiple Roughness Characteristics of Chemically Deposited Ni-P-W Coatings," *Tribol. Ind.*, vol. 34, no. 4, pp. 186–197, 2012.

[33] O.I. Abdullah, J. Schlattmann and A.M. Al Shabibi, "Stresses and Deformations Analysis of a Dry Friction Clutch System," *Tribolology in Industry*, vol. 35, no. 2, pp. 155–162, 2013.